Heliyon

Received:
27 January 2017
Revised:
13 April 2017
Accepted:
25 May 2017

Cite as: Brandy J. Johnson, Anthony P. Malanoski, Jeffrey S. Erickson, Ray Liu, Allison R. Remenapp, David A. Stenger, Martin H. Moore. Reflectance-based detection for long term environmental monitoring. Heliyon 3 (2017) e00312.
doi: 10.1016/j.heliyon.2017.e00312

Reflectance-based detection for long term environmental monitoring

Brandy J. Johnson [a,*], Anthony P. Malanoski [a], Jeffrey S. Erickson [a], Ray Liu [b,1], Allison R. Remenapp [c,2], David A. Stenger [a], Martin H. Moore [a]

[a] *Center for Bio/Molecular Science and Engineering, Naval Research Laboratory, Washington, DC 20375 USA*

[b] *Thomas Jefferson High School for Science and Technology, Alexandria, VA 22312 USA*

[c] *Department of Chemistry, Washington College, Chestertown, MD 21620 USA*

* Corresponding author.

E-mail address: brandy.white@nrl.navy.mil (B.J. Johnson).

[1] at NRL through SEAP

[2] at NRL summer 2016

Abstract

Here, the potential of colorimetric sensors utilizing porphyrin indicators for long term environmental monitoring is demonstrated. Prototype devices based on commercial color sensing chips (six per device) were combined with in-house developed algorithms for data analysis. The devices are intended to provide real-time sensing of threats. An initial outdoor data set was collected using prototype devices with occasional spiked exposure to targets. This data was supported by similar data collected in a controlled indoor environment. Weaknesses in the noted performance of the devices during these experiments were addressed through altering device parameters, algorithm parameters, and array element composition. Additional outdoor data sets totaling 1,616 h and indoor data sets totaling 728 h were collected in support of assessing these changes to the system configuration. The optimized system provided receiver operating characteristics (ROC) of specificity 0.97 and sensitivity 1.0.

Keyword: Environmental science

http://dx.doi.org/10.1016/j.heliyon.2017.e00312

1. Introduction

The development of sensor platforms for environmental monitoring or surveillance is an ongoing area of interest. With the increased availability of connectivity technologies (cellular/WiFi) and continuing advances in supporting hardware and software, generation of consensus decisions based on distributed sensors has become more feasible [1, 2, 3, 4]. It remains true that platform development is faced with serious design constraints on power and size as well as sensor specificity and sensitivity. An additional challenge stems from the envisioned applications in which different types of information may be important. For instance, the design criteria for detailed monitoring of concentrations for a single gas target are very different from the requirements for broad spectrum monitoring of many gases at threshold levels. While sensors developed for the single gas task could be applied to the second task, there will likely be a cost imposed by capabilities that are not required, and additional complexity would be expected in coordinating many individual sensors applicable to the range of targets of interest in the second application.

Sensor methodologies are being explored to achieve a broader range of applications: remote sensing, arrays of indicators (artificial nose/tongue), and, more recently, multivariable sensor approaches [5, 6, 7, 8, 9, 10, 11]. Potyrailo [10] provides a comprehensive review of several sensor technologies and compares several sensing approaches. Standoff detection presents a compromise with a few units can covering an area of interest; however, the cost and operational requirements of an individual unit remain high [12]. The approaches also remain limited to line of sight and continue to suffer from background interference. Significant effort has been invested in the development array based sensing approaches, including various chemical sensing modes and methods to maximize the information obtained from arrays [5, 6, 7, 13]. Implementations include both electrochemical and optical approaches [5, 6, 12, 14, 15]. Optical methods range from image capture with post processing to simple color intensity measurements [6, 7, 16, 17, 18, 19]. The indicators for these sensors often use semiselective interactions to allow for long term and broad spectrum application, resulting in challenges for discrimination of targets. Various approaches have been explored as a means of addressing the cost, power, and effectiveness of the final device. Multivariable sensors represent a more recent area of research that attempts to overcome specificity issues inherent in array approaches through interrogation of an indicator element in several ways. This is a relatively new approach; the technologies tend to be less mature than the available array and standoff approaches [10].

Our focus has been on development of sensors for threshold monitoring of multiple targets [9, 13, 20]. The ongoing effort has prompted significant exploration of

http://dx.doi.org/10.1016/j.heliyon.2017.e00312

methods to process information from arrays of indicators in order to mitigate the shortcomings of individual elements and to obtain a rapid consensus result from the large amount of available information. It remains that there are no sensor systems available for multiple, simultaneous target monitoring in a low cost, low power format. While several array based technologies are being developed, they typically require relatively intense data processing (image processing or spectrophotometric analysis), increasing cost and power requirements. We have chosen to focus on a simplified information stream, utilizing only the reflectance intensity of the indicator elements. We have demonstrated selection of effective arrays for some targets and the basic concept of device utilization [9, 20]. The use of porphyrins as indicator elements provides strong colorimetric changes with discrimination achieved through the use of different chemical structures and incorporation of metal sites. The use of reflectance responses lowers cost and power requirements for the devices. Recognizing that the goal of the application is threshold detection alters the mode in which we operate the array devices. The concentrations of detected targets are not the point of interest; rather, the devices are intended to provide an indication of target presence above threshold levels. We have established a detection algorithm focused on this goal [13]. The algorithm effectively compensates for general background interference. It is also computationally simple, keeping device power requirements to a minimum [13].

The current study provides long term utilization of the prototype devices and the associated algorithm under outdoor conditions, providing data necessary for further refinement of both. The largest pool of interferents for sensors used in urban settings are the various gases produced from automobiles and industrial processes and the natural diurnal variations in humidity and temperature. This effort deployed prototype devices for unattended periods of up to 14 days with occasional introduction of target, simulating exposure events. The study identified shortfalls in prototype operational parameters and allowed for further optimization of the algorithm utilized.

2. Materials and methods

Silver (AgN_4TPP) and zinc (ZnN_4TPP) variants of meso-tetra(4-aminophenyl) porphine (CAS 22112-84-1) and silver (AgDIX), yttrium (YtDIX), and thallium (TlDIX) variants of Deuteroporphyrin IX bis ethylene glycol (CAS 6239456-72-5) were prepared by reflux as previously reported [9, 20]. Paper supported porphyrin indicators were prepared using a dip and dry technique [13, 20]. For a 5 × 33 cm swatch, 0.4 mM porphyrin in water (total volume 6 mL) was used. The paper support (WypAll X60) was pulled through this solution and allowed to dry slightly before being pulled through the solution again. This was repeated until all porphyrin solution had been deposited (typically three cycles). Samples were then dried at 100 °C before storing in the dark in sealed plastic bags.

http://dx.doi.org/10.1016/j.heliyon.2017.e00312

2.1. Prototype devices

The PT3 prototype reflectance instrument utilized low cost, commercially available color sensing breakout boards from Parallax, Inc. (model TCS3200-DB, Rocklin, CA), providing a color light-to-frequency integrated circuit from AMS (model TCS3200, Plano, TX), a pair of white LEDs, and an adjustable lens. The device was previously described in detail [9]. Briefly, six of the breakout boards were used with a customized multiplex platform in which the boards were mounted using in-house developed holders made from chemically resistant Delrin plastic (McMaster-Carr, Princeton, NJ). The device output consists of a stream of digital pulses proportional to the intensity of the color being measured. A custom printed circuit board (PCB) interfaces with and controls the six sensors. The PCB uses an Atmel ATMega microcontroller (Atmel Corporation, San Jose, CA) to regulate the timing of events, count pulses, and report the results to a computer. Communications between the instrument and the computer are via USB; power is supplied through a dc barrel jack. A LabWindows developed software-based graphical user interface (GUI) communicates with the PCB firmware through simple ASCII commands.

The PT4 prototype is a modified version of the PT3 device [9, 13, 20]. Like the PT3, the heart of this instrument is the TCS-3200-DB breakout board (Parallax). The stock version of this board includes a color sensor (TCS-3200, AMS), an adjustable lens, and white LEDs. Peak sensitivity for the TCS-3200 sensor occurs at 470 nm, 524 nm, and 640 nm. Because the cool white LEDs used in this board have low emission in the red portion of the spectrum, one of the white LEDs on each detector board was replaced with a 636-nm red LED rated at 1800 mcd at 20 mA forward current (Lumex, product #SSL-LX5093SIC). This replacement enhances performance over the red region of the spectrum. The two LEDs are aligned to the center of a target placed 25.4 mm away from the board prior to installation in the instrument. PT4 includes six TCS-3200-DB boards modified as described above. Detectors are sequentially mounted onto the top rails of a black plastic sample holder machined from chemically resistant Delrin (Fig. 1). Porphyrin samples are mounted at the bottom of the holder with spring clips, 25.4 mm from the detectors. After mounting these parts, the sample holder forms a rectangular tube. Airflow through this tube at 2.7CFM is provided by two small 5 VDC fans (Orion Fans, model #OD2510-05HB), one mounted at each end.

The instrument housing is designed for outdoor use. The housing is machined from chemically resistant Delrin plastic (McMaster-Carr) and secured with 316-Stainless Steel screws. Black plastic was chosen to minimize stray reflections. Plastic tipped thumb screws are used to seal the top of the instrument. All of the holes in the housing, for cords and for sample airflow, are located on the bottom of the instrument to protect from water penetration. The housing contains the sample

http://dx.doi.org/10.1016/j.heliyon.2017.e00312

Fig. 1. Photographs of the prototype devices: (a) device in outdoor, simulated forest environment; (b) detail of device components; (c) device on roof top at ~18 m; (d) device on roof top at ~11 m.

holder; the fans; and a home-built circuit board that provides power management, data acquisition, on-board flash memory, and control of the individual sensors. Two separate power lines are required for operation, one for the fans at 5 VDC and a second for the control board at 7.5 VDC. USB interface allows for connection of the instrument to a computer. The instrument is designed to run autonomously for a duration of 7 days. The firmware controlling the instrument is similar to that described for PT3, with the exception of the added flash memory functionality. A laptop computer equipped with custom software (written in LabWindows) is used to start and stop each experiment and to download data from the instrument but is not required to be connected during the seven day deployment. Data acquired in real time is stored on flash memory and downloaded to the laptop over the USB connection after completion of the experiment.

The studies reported here utilized three PT4 devices. Each device was mounted on a heavy duty plastic milk crate and secured with nylon cable ties (Fig. 1). All outdoor deployments were completed in Washington, DC, USA. The first deployment site is a rooftop approximately 11 m above grade. The second site is also a rooftop, approximately 18 m above grade. The third site is at ground level in a simulated highland forest environment (outdoor experimental facility). Supporting data on temperature and humidity during use of the instruments, were collected using co-located devices (Omega Portable Data Logger with USB interface; OM-EL-USB-1). For data collected in a glove enclosure (65 L; Techni-Dome, Bel-Art, Wayne, NJ,

http://dx.doi.org/10.1016/j.heliyon.2017.e00312

USA), the volume was continuously purged using humidified air. This condition was used during establishment of baseline measurements. Exposures were accomplished by adding a fixed volume of target to the continuous air stream.

Here, the initial data set is comprised of 19,597 h of run time with 15,826 h of outdoor use and 3,771 h of laboratory use. Outdoor use includes: 5,989 h at the 11 m site, 4,607 h at the 18 m site, and 5,230 h in the highland forest environment. Exposure events include 72 target and interferent applications (432 individual indicator exposures); 24 of these events were completed in outdoor environments (144 indicator exposures). Exposures were completed using two approaches. The first type used a syringe to aerosolize the target in a 0.8 m^2 area surrounding the prototype device. The total volume used was 200 mL with a delivery time of 3 min. The second type used a target saturated glass fiber filter of diameter 5.5 cm (Whatman) placed against the inlet fan. Performance differences between the two exposure types were not observed. Follow-on data is comprised of 1,056 h collected at the 18 m site (264 h at each of four integration durations) with 36 exposure events and 1,148 h of indoor data (287 h at each of four integration durations) with 48 exposure events. For access to raw data, please contact the corresponding author at brandy.white@nrl.navy.mil.

2.2. Data analysis

The algorithm utilized for analysis of the data sets has been described in detail [13]. Briefly, anomalous values resulting from a rare reporting error (Fig. 2) were excluded in the first round of processing by comparing the channel value (red, green, blue of a given indicator) to that reported for the previous time point. If the absolute value of the difference between the two divided by the previous value was greater than 35%, the previous value was substituted for the current value. A threshold angle for a detection event is fixed based on the first 120 data points

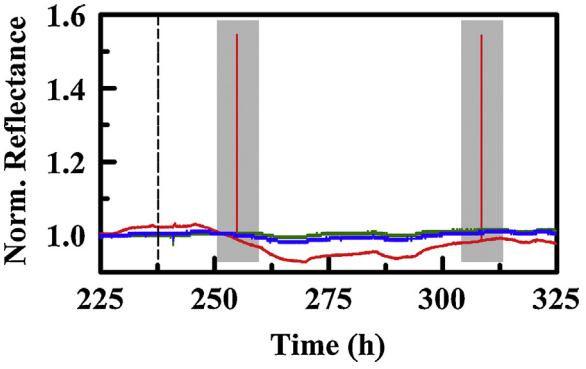

Fig. 2. Example of instrument reporting error (highlighted gray region). This data set is YtDIX in the PT4 prototype under laboratory conditions. Dashed line indicates beginning of exposure to 1,1-difluoroethane.

http://dx.doi.org/10.1016/j.heliyon.2017.e00312

collected by the device. Linear regression formulas are used to compute slope and r^2 values for each color channel of each indicator (R, G, and B times six indicators) for the current window (most recent 20 data points) and the background window (next 120 most recent points). The cosine of the angle between the slopes is compared to the threshold value to identify the occurrence of an event. An additional window of the 10 most recent data points requires changes on a larger scale for identification of rapidly occurring events. The algorithm can be varied to report an event based on changes at a single indicator (s1), two indicators (s2), or three indicators (s3). The initiation of an event opens a window of 60 mins during which any changes are considered part of the initial event; this window closes 60 min after the last changes meeting the established criteria.

3. Results

Our previous report [9] detailed the performance of an initial prototype. Based on those results a new generation prototype (PT4) was developed for evaluation of the sensing approach in outdoor environments. The array elements (6 per device) were selected based on the results of the initial effort with the PT3 device [9]. These elements, AgN_4TPP, ZnN_4TPP, AgDIX, YtDIX, and TlDIX, provided differential responses to the alcohol targets selected for demonstration purposes: ethanol, methanol, and isopropanol. Fig. 3 compares the response of the PT3 device to that of PT4 in an experiment in which the two devices are simultaneously exposed to ethanol in a glove enclosure. Differences in the presented RGB profiles are the result of differences in breakout board production lots and the replacement of one white LED illumination source on each chip with a red LED in the PT4 devices (see Section 2). It should be noted that the sampling increment was increased from

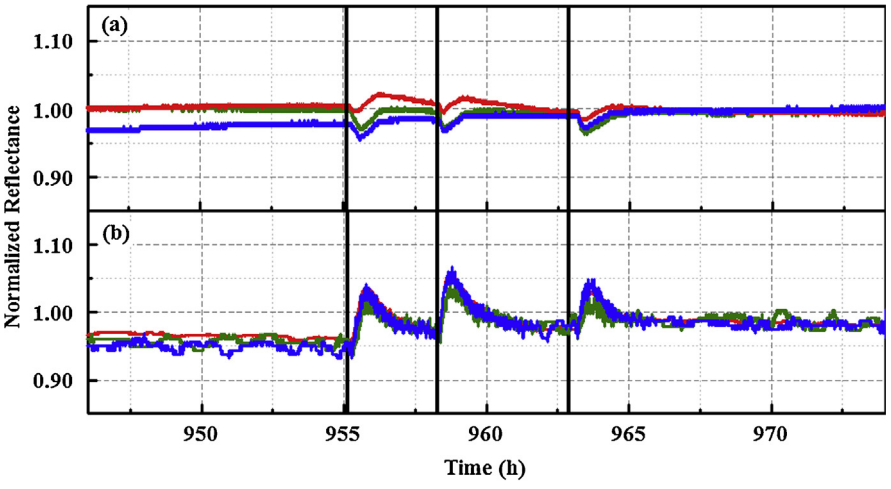

Fig. 3. Response of AgN_4TPP indicator to ethanol exposure (1.06 ppm) in a laboratory environment as reported by (a) PT3 and (b) PT4. Normalized red, green, and blue (RGB) color values are presented for each device. Black lines indicate the initiation of an exposure event.

http://dx.doi.org/10.1016/j.heliyon.2017.e00312

5 s for PT3 to 30 s for PT4, allowing for longer periods of autonomous function (up to 7 days).

3.1. Deployment of the PT4 devices

The three PT4 devices were placed at three outdoor sites to collect data over long duration with periodic data download. Sites were selected to provide variations in exposure conditions. The simulated highland forest environment provides a site in close proximity to a water source (man-made pond) as well as exposure to changing factors introduced by the seasonal cycle of the trees and plants. Insect and wildlife actions also contribute to this environment. The 11 m rooftop site provides a sheltered situation; there is exposure to weather but the device is partially shielded from wind. The final site, a roof top at 18 m, is exposed to weather and has more direct wind exposure. It is also located in proximity to building service components, including fume hood exhaust stacks and heating, ventilating, and air conditioning components (HVAC). Fig. 4 provides an excerpt of a data set; representative data sets for long term outdoor use are provided in Fig. 5 and Fig. 6. As shown, the reported indicator values change in response to diurnal shifts in temperature and humidity. Laboratory experiments indicate that this change is related to humidity rather than temperature (Fig. 7).

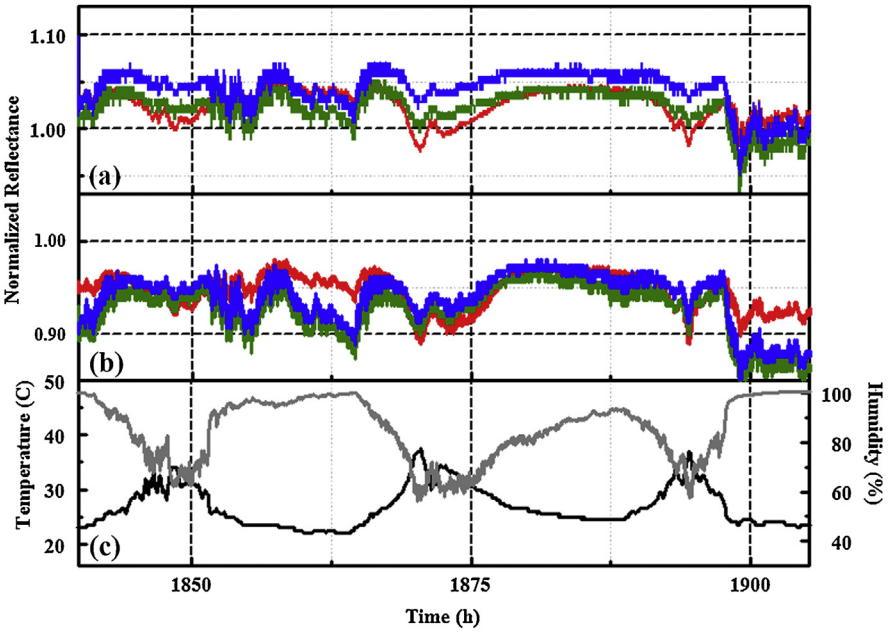

Fig. 4. Red, green, and blue (RGB) profiles for PT4 collected in the simulated highland forest environment July 6 to 8, 2015. Response of (a) ZnN_4TPP and (b) AgDIX to environmental variations. Temperature (black) and humidity (gray) as recorded by a co-located device are also provided (c). This data is excerpted from Fig. 5.

http://dx.doi.org/10.1016/j.heliyon.2017.e00312

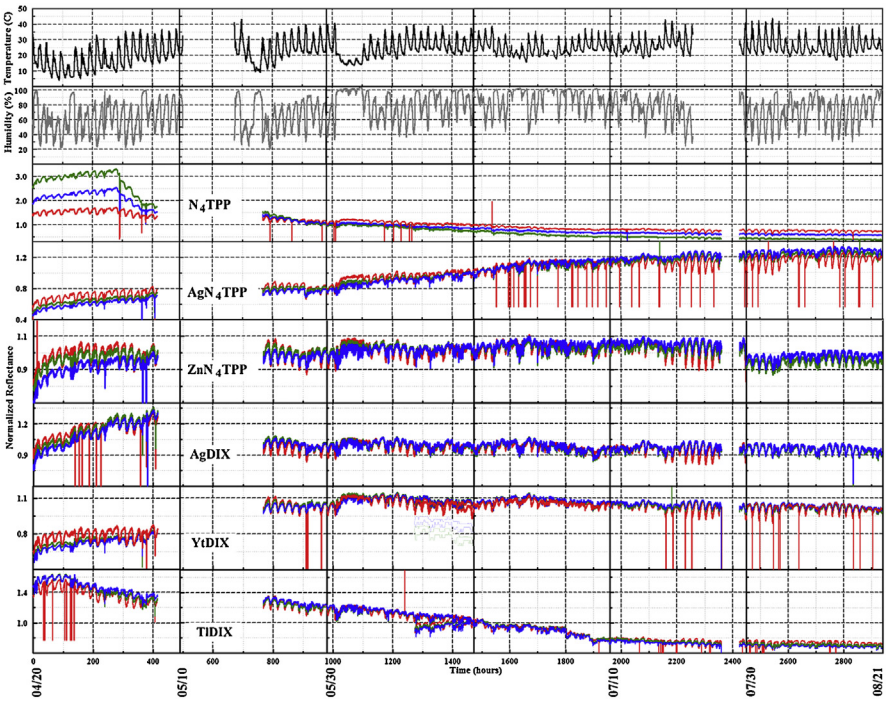

Fig. 5. Normalized RGB color value data set collected in the simulated highland forest environment between April 20 and August 20, 2015. Temperature and humidity as reported by a co-located device are also provided.

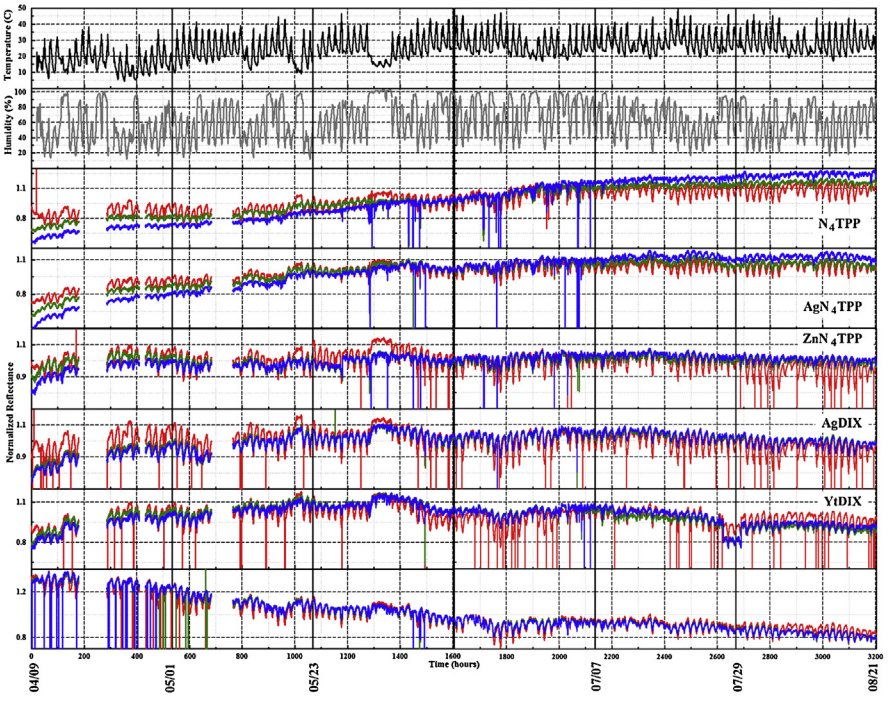

Fig. 6. Normalized RGB color value data set collected on the 11 m rooftop between April 9 and August 21, 2015. Temperature and humidity as reported by a co-located device are also provided.

http://dx.doi.org/10.1016/j.heliyon.2017.e00312

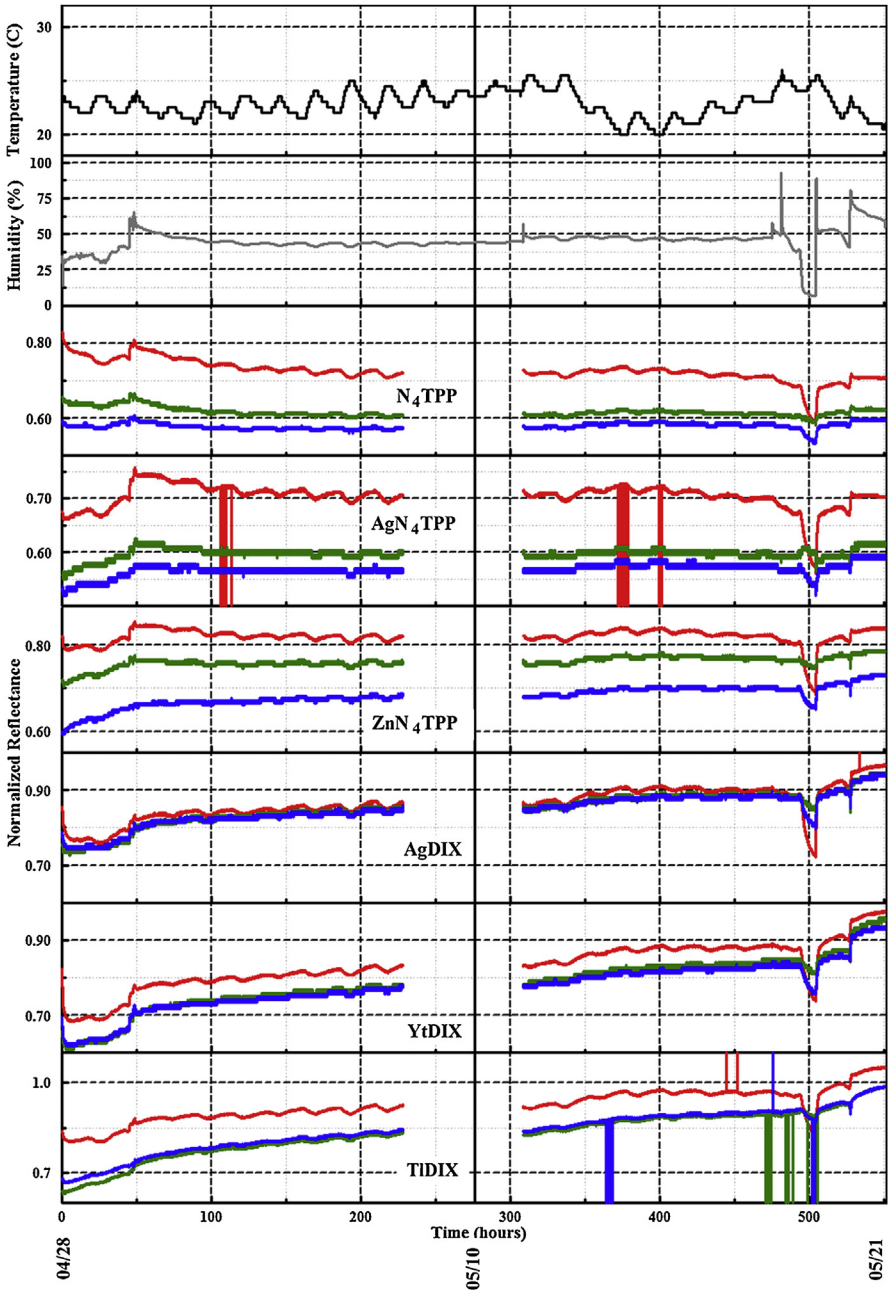

Fig. 7. Normalized RGB color value data set collected in the laboratory environment between April 28 and May 21, 2015. Temperature (black) and humidity (grey) as reported by a co-located device are also provided.

Based on the data collected by the PT4 devices in outdoor environments, the single indicator algorithm (s1) reported a number of events that were not associated with alcohol exposures (Fig. 8; full data set, Fig. 6). Using the 2,937 h data set collected in the forest environment (April 20 to August 20), the time difference between the first criteria meeting change in the window and the last for 47% of events is less

http://dx.doi.org/10.1016/j.heliyon.2017.e00312

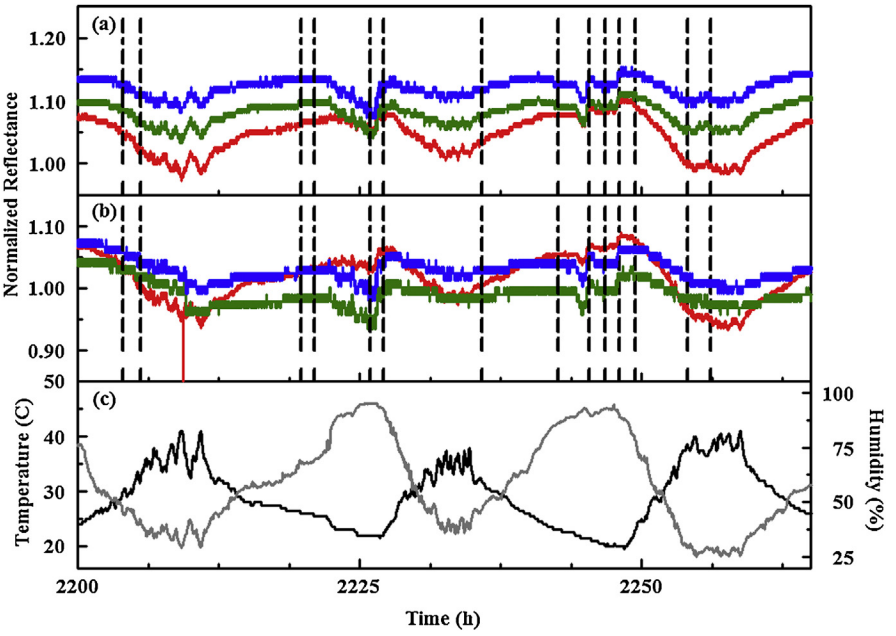

Fig. 8. Red, green, and blue (RGB) profiles for PT4 collected at a rooftop location (11 m) July 10 to 12, 2015. Response of (a) AgN_4TPP and (b) YtDIX to environmental variations. Temperature (black) and humidity (gray) as recorded by a co-located device are also provided (c). Dashed lines indicate events reported by the algorithm (s1). This data is excerpted from Fig. 6.

than 5 min (Table 1). All of the indicators are involved in multiple identified events; there are a total of 390. The median event length is 11 min; the average is 46 min. Full results as well as results for additional device deployments are summarized in Table 1. On average, the outdoor deployments resulted in one false positive event every 6.5 h. Some differences were noted between the sites; the average time between false positive events was 10 h for the 18 m rooftop site, 4 h for the 11 m rooftop site, and 5.5 h for the forest site.

Fig. 9 provides a comparison of temperature and humidity data for the 11 m rooftop site to that of the forest site for the same time period. Small changes in humidity occur over short time scales in the forest environment; these types of events are less predominant in data from the rooftop device. Changes in both temperature and humidity, when considered on a daily basis, are more extreme for the rooftop device, with higher rates of change also observed. This is likely a result of full sun exposure and the reflection of heat from the surrounding structures. The events identified by the algorithm, however, cannot be associated to features in the profile of humidity or temperature for any of the devices. The algorithm was designed to capture events occurring over short time scales. The detection window uses 20 points covering a 10 min period. The indicator responses to changing humidity occur over much longer time periods.

http://dx.doi.org/10.1016/j.heliyon.2017.e00312

http://dx.doi.org/10.1016/j.heliyon.2017.e00312

Table 1. Summary of single seat algorithm (s1) results and ROC analysis for the sensor deployments considered under this study.

Location	Duration	Exposures*	Events	Events < 5 min	Median Length (min)	Mean Length (min)	True Positives	False Positives	False Negatives	True Negatives	Specificity	Sensitivity
Rooftop, 18 m	495	5	84	19	23	59	4	80	0	377	0.82	1.00
Rooftop, 11 m	606	4	80	11	25	64	4	76	0	487	0.87	1.00
Forest	906	3	194	82	13	45	2	192	1	671	0.78	0.67
Laboratory	332	10	7	0	60	45	6	1	4	322	1.00	0.60
Rooftop, 11 m	330	0	24	5	53	70	0	24	0	293	0.92	
Forest	94	0	24	11	7	38	0	24	0	67	0.74	
Laboratory	583	4	3	2	22	29	2	1	2	578	1.00	0.50
Laboratory	586	7	3	3	60	40	1	2	6	640	1.00	0.14
Laboratory	633	5	0	–	–	–	0	0	5	626	1.00	0.00
Laboratory	99	2	1	2	2	2	1	0	1	98	1.00	0.50
Laboratory	99	1	2	2	2	2	1	1	0	98	0.99	1.00
Laboratory	95	0	0	–	–	–	0	0	0	95	1.00	
Rooftop, 11 m	527	5	65	31	8	40	4	61	1	449	0.88	0.80
Forest	529	3	69	15	20	56	2	66	0	433	0.87	1.00
Laboratory	793	9	6	3	18	24	5	1	1	788	1.00	0.83
Rooftop, 11 m	3203	0	452	184	14	47	0	452	0	2646	0.85	
Forest	2937	0	390	175	11	46	0	390	0	2461	0.86	
Laboratory	551	5	4	0	59	50	3	1	2	543	1.00	0.60
Rooftop, 18 m	2747	0	290	59	33	79	0	290	0	1655	0.85	
Rooftop, 18 m	653	3	71	25	17	46	3	68	0	561	0.89	1.00
Rooftop, 18 m	450	0	24	10	15	48	0	24	0	419	0.95	
Forest	429	0	66	38	4	23	0	66	0	1113	0.94	
Rooftop, 11 m	988	1	76	37	6	37	0	76	1	905	0.92	0.00
Rooftop, 18 m	262	0	0	–	–	–	0	0	0	261	1.00	

(*Continued*)

Table 1. (*Continued*)

Location	Duration	Exposures*	Events	Events < 5 min	Median Length (min)	Mean Length (min)	True Positives	False Positives	False Negatives	True Negatives	Specificity	Sensitivity
Forest	335	0	38	19	5	23	0	38	0	317	0.89	
Rooftop, 11 m	335	0	6	3	12	35	0	6	0	331	0.98	

* Includes target and interferent exposures.

http://dx.doi.org/10.1016/j.heliyon.2017.e00312

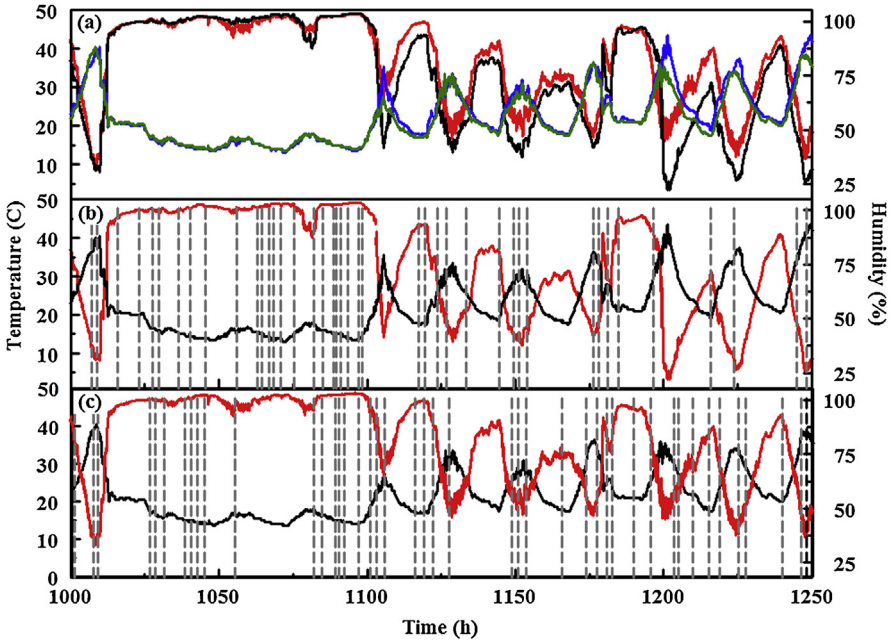

Fig. 9. Temperature and humidity (a) values collected at the forest (green and red, respectively) and 11 m rooftop (blue and black, respectively) sites between June 1 and 11, 2015. (b) Data for rooftop site (temperature, black and humidity, red) is shown in comparison to events identified by the algorithm (gray). (c) Data for forest site (temperature, black and humidity, red) is shown in comparison to events identified by the algorithm (gray). Dashed lines indicate the beginning of event windows. Total event window time for the period shown is 34 h for the forest device and 36.2 h for the rooftop device.

Use of the devices in the laboratory environment resulted in significantly fewer false reporting events. For the laboratory data sets collected under this study, there was, on average, one reported false positive for every 527.5 h of operation. These units were exposed to the ambient atmosphere in a laboratory, with minimal changes in temperature and humidity. The representative data presented included 551 h with five ethanol exposures at 0.4 ppm (Fig. 7; excerpt in Fig. 10). Calculation of sensitivity and specificity based on the approach used by the receiver operating characteristic (ROC) provides a simple method for comparison of device and algorithm performance. Specificity is calculated as the ratio of the true negative responses to the sum of the true negative and false positive responses. Sensitivity is calculated as the ratio of the true positive responses to the sum of the true positive and false negative responses. Analysis of the total laboratory dataset indicates specificity 1.0 and sensitivity 0.48. For comparison, analysis of overall performance in outdoor environments yields a specificity of 0.87 and sensitivity 0.86 (Table 2); Table 1 provides results separated by individual experiment. Indoor exposures utilized a range of alcohol concentrations as well as potential interferent compounds: methyl salicylate, acetone, Simple Green®, peppermint oil (Po-Ho Oil, A. Vogle), naphthalene, and 1,1-diflurorethane. Outdoor exposures focused on

http://dx.doi.org/10.1016/j.heliyon.2017.e00312

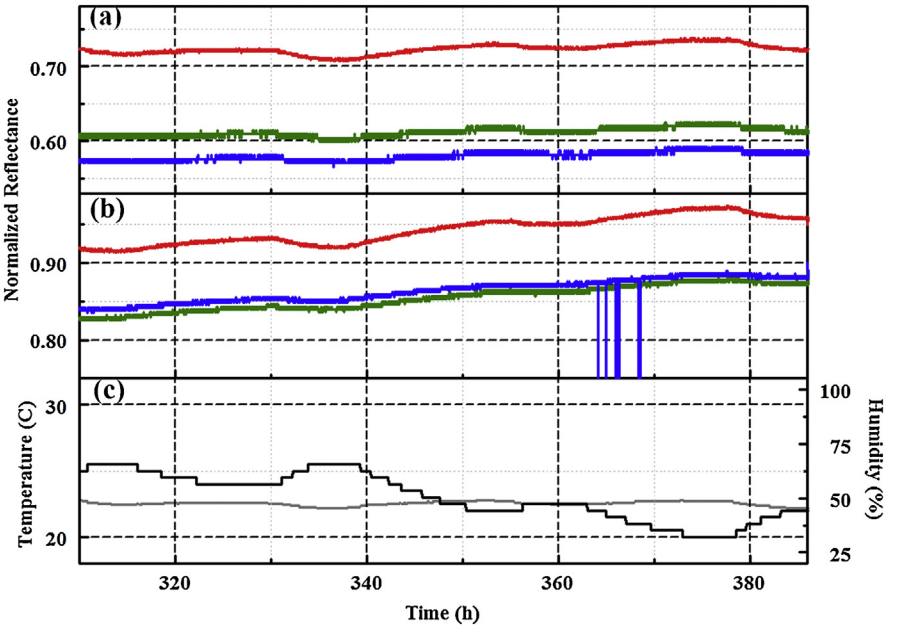

Fig. 10. Red, green, and blue (RGB) profiles for PT4 collected in the laboratory May 4 to 6, 2015. Response of (a) N_4TPP and (b) TlDIX to environmental variations. Temperature (black) and humidity (gray) as recorded by a co-located device are also provided (c). This data is excerpted from Fig. 7.

ethanol. These differences can explain the variations in sensitivity noted; however, changes in specificity are related to the complexities of the outdoor environment.

3.2. Adjusting algorithm parameters

Given the loss in specificity observed when moving from indoor to outdoor device utilization, adjustments were made to the algorithm. Initial sensitivity thresholds were designed based on the PT3 device [9]. Previous work included some optimization designed to accommodate the difference in performance of the PT4 device;[13] however, data from environmental deployment was not considered.

Table 2. Summary of ROC analysis based on single seat algorithm (s1) results for the sensor deployments considered under this study. Results by experiment provided in Table 1.

Location	True Positives	False Positives	False Negatives	True Negatives	Specificity	Sensitivity
Total Overall	38	1940	24	17234	0.90	0.61
Total Laboratory	19	7	21	3788	1.00	0.48
Total Outdoor	19	1933	3	13446	0.87	0.86
Total Rooftop, 18 m	7	462	0	3273	0.88	1.00
Total Rooftop 11m	8	695	2	5111	0.88	0.80
Total Forest	4	776	1	5062	0.87	0.80

http://dx.doi.org/10.1016/j.heliyon.2017.e00312

Rather, all data utilized in algorithm development was collected within a glove enclosure providing controlled temperature and humidity as well as controlled target exposures [13]. As shown above, events reported for data from outdoor sites result from changes in environmental conditions aside from temperature and humidity. It is possible that some of these events are related to significant changes in the chemical composition of the air sampled; however, given the large number of events reported, it is likely that most are false responses that should be excluded from the reported results.

The algorithm was adjusted using several approaches. Previously, requirements for changes on two (s2) or three (s3) of the six indicators were considered [13]. This requirement also included a change to the threshold values used in event discrimination in an attempt to optimize the balance between sensitivity and specificity ($\theta = 70*\exp(-RGB/30) + c$). The c parameter is set for each indicator separately and is the larger value of a default (0.45) in the original parameter setting or the value of the standard deviation of the color channel for that sensor. For algorithm variations s3th1 and s3th2, c parameter default minimum threshold values of 1 and 2, respectively, were used. Table 3 presents results for the full data set considered under this study using these algorithm variations. As shown, the original multi-indicator requirements resulted in losses in sensitivity with little improvement in specificity for the dataset. Algorithm variations s3th1b and s3th2b utilized the three indicator requirement with the less sensitive threshold value utilized under the s1 algorithm ($\theta = 20*\exp(-RGB/130) + c$) and c parameter default minimum threshold values of 1 and 2, respectively. As shown in Table 3, the specificity of the results can be improved through these types of variations to the algorithm, but the improvements are at the expense of sensitivity.

3.3. Adjusting device parameters

Our previous work has included studies focused on the indicator support, total porphyrin loading, and indicator selection as well as on development of the described algorithm [9, 13, 20]. The device hardware has also been modified to provide improved coverage of the red region of the visible spectrum by the illumination sources [13]. Based on the limited overall gains achieved through modification of algorithm parameters, the current effort evaluated the impact of modifications to the operational parameters of the prototype device. The data reported for PT4 above was collected using a 30 s sampling interval with 100 ms integration. Under laboratory utilization, as presented above, it was possible to obtain a specificities of 1.0 using even the s1 algorithm, though sensitivities were only 0.5.

An additional data set was collected in which four devices were placed in an enclosure providing controlled temperature and humidity. The devices utilized four

http://dx.doi.org/10.1016/j.heliyon.2017.e00312

Table 3. Summary of algorithm reporting for the total dataset considered under this study and the subgroupings of data.

Algorithm Variation	True Positives	False Positives	False Negatives	True Negatives	Specificity	Sensitivity
Complete Dataset						
S1	38	1940	24	17234	0.90	0.61
S2	38	2140	23	16450	0.88	0.62
S3	35	1784	26	17374	0.91	0.57
S3th1	20	971	30	16463	0.94	0.40
S3th2	17	553	44	19283	0.97	0.28
S3th1b	15	426	47	19076	0.98	0.24
S3th2b	12	144	50	19317	0.99	0.19
Laboratory (Total)						
S1	19	7	21	3788	1.00	0.48
S2	20	4	19	3788	1.00	0.51
S3	17	5	22	3790	1.00	0.44
S3th1	13	3	26	3824	1.00	0.33
S3th2	6	0	34	3835	1.00	0.15
S3th1b	7	0	33	3836	1.00	0.18
S3th2b	4	0	36	3837	1.00	0.10
Outdoors (Total)						
S1	19	1933	3	13446	0.87	0.86
S2	18	2136	4	12662	0.86	0.82
S3	18	1779	4	13584	0.88	0.82
S3th1	7	935	3	12138	0.93	0.70
S3th2	11	540	9	14921	0.97	0.55
S3th1b	8	423	13	14703	0.97	0.38
S3th2b	8	144	13	14943	0.99	0.38
Rooftop, 18 m						
S1	7	462	0	3273	0.88	1.00
S2	7	497	0	3137	0.86	1.00
S3	7	461	0	3301	0.88	1.00
S3th1	2	251	1	3195	0.93	0.67
S3th2	3	104	3	3917	0.97	0.50
S3th1b	1	153	6	3867	0.96	0.14
S3th2b	2	34	5	3995	0.99	0.29
Rooftop, 11 m						
S1	8	695	2	5111	0.88	0.80
S2	7	744	3	4907	0.87	0.70
S3	7	572	3	5283	0.90	0.70

(*Continued*)

http://dx.doi.org/10.1016/j.heliyon.2017.e00312

Table 3. (*Continued*)

Algorithm Variation	True Positives	False Positives	False Negatives	True Negatives	Specificity	Sensitivity
S3th1	3	333	2	5045	0.94	0.60
S3th2	5	159	4	6032	0.97	0.56
S3th1b	5	90	4	5730	0.98	0.56
S3th2b	4	41	5	5732	0.99	0.44
Forest						
S1	4	776	1	5062	0.87	0.80
S2	4	895	1	4618	0.84	0.80
S3	4	746	1	5000	0.87	0.80
S3th1	2	351	0	3898	0.92	1.00
S3th2	3	277	2	4972	0.95	0.60
S3th1b	2	180	3	5106	0.97	0.40
S3th2b	2	69	3	5216	0.99	0.40

different integration durations for data collection: 100, 300, 400, and 500 ms; 500 ms is the upper limit for integration in the current prototype based on a 30 s sampling interval (Fig. 11). Exposures to ethanol, methanol, and isopropanol in concentrations from 0.12 to 2.28 ppm were completed. Table 4 presents a summary of the results following analysis by the s1 algorithm. As shown, increasing the integration time to 400 ms provided specificity and sensitivity equal to 1.0 under these conditions. The devices were moved to an outdoor environment for

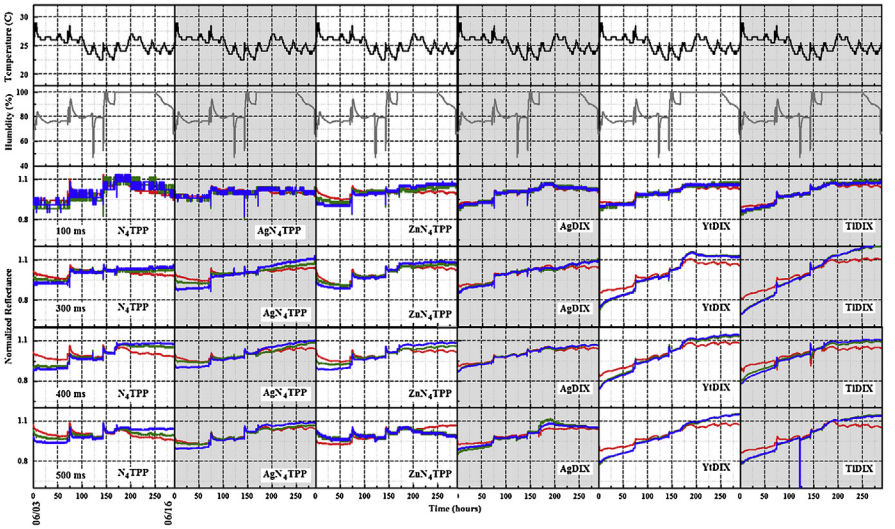

Fig. 11. Normalized RGB color value data set collected in the laboratory environment between June 3 and June 16, 2016 at 100, 300, 400, and 500 ms integration. Temperature (black) and humidity (grey) as reported by a co-located device are also provided.

http://dx.doi.org/10.1016/j.heliyon.2017.e00312

Table 4. Results for analysis of data collected at varied integration.

Algorithm Variation	True Positives	False Positives	False Negatives	True Negatives	Specificity	Sensitivity
Laboratory, 100 ms						
S1	4	6	5	157	0.96	0.44
S2	5	0	4	164	1.00	0.56
S3	4	0	5	163	1.00	0.44
S3th1	4	0	5	164	1.00	0.44
S3th2	2	0	7	557	1.00	0.22
S3th1b	2	0	7	161	1.00	0.22
S3th2b	2	0	7	161	1.00	0.22
Laboratory, 300 ms						
S1	7	0	2	165	1.00	0.78
S2	7	0	2	165	1.00	0.78
S3	6	0	3	164	1.00	0.67
S3th1	5	0	4	163	1.00	0.56
S3th2	3	0	6	162	1.00	0.33
S3th1b	3	0	6	162	1.00	0.33
S3th2b	1	0	8	160	1.00	0.11
Laboratory, 400 ms						
S1	9	0	0	158	1.00	1.00
S2	9	0	0	160	1.00	1.00
S3	8	0	1	161	1.00	0.89
S3th1	6	0	3	164	1.00	0.67
S3th2	3	0	6	162	1.00	0.33
S3th1b	5	0	4	163	1.00	0.56
S3th2b	3	0	6	162	1.00	0.33
Laboratory, 500 ms						
S1	8	1	1	160	0.99	0.89
S2	9	0	0	164	1.00	1.00
S3	7	0	2	163	1.00	0.78
S3th1	5	0	4	163	1.00	0.56
S3th2	3	0	6	162	1.00	0.33
S3th1b	5	0	4	163	1.00	0.56
S3th2b	1	0	8	160	1.00	0.11
18 m roof, 100 ms						
S1	7	19	5	95	0.83	0.58
S2	4	7	8	173	0.96	0.33
S3	3	6	9	175	0.97	0.25
S3th1	3	6	9	159	0.96	0.25

(*Continued*)

http://dx.doi.org/10.1016/j.heliyon.2017.e00312

Table 4. (*Continued*)

Algorithm Variation	True Positives	False Positives	False Negatives	True Negatives	Specificity	Sensitivity
S3th2	1	2	11	159	0.99	0.08
S3th1b	1	2	11	159	0.99	0.08
S3th2b	0	0	12	161	1.00	0.00
18 m roof, 300 ms						
S1	12	19	0	87	0.82	1.00
S2	12	21	0	75	0.78	1.00
S3	12	22	0	78	0.78	1.00
S3th1	10	8	2	135	0.94	0.83
S3th2	2	5	10	136	0.96	0.17
S3th1b	2	5	10	136	0.96	0.17
S3th2b	1	5	11	136	0.96	0.08
18 m room, 400 ms						
S1	12	28	0	56	0.67	1.00
S2	12	26	0	56	0.68	1.00
S3	12	23	0	62	0.73	1.00
S3th1	9	16	3	101	0.86	0.75
S3th2	5	6	7	155	0.96	0.42
S3th1b	5	6	7	155	0.96	0.42
S3th2b	5	4	7	157	0.98	0.42
18 m roof, 500 ms						
S1	11	27	1	78	0.74	0.92
S2	11	26	1	82	0.76	0.92
S3	10	19	2	86	0.82	0.83
S3th1	8	4	4	162	0.98	0.67
S3th2	2	1	10	229	1.00	0.17
S3th1b	2	1	10	229	1.00	0.17
S3th2b	1	0	11	230	1.00	0.08

comparison of the integration durations under the more variable conditions (Fig. 12). As shown in Table 4, the s1 algorithm yielded high false positive rates regardless of the integration time used. At 300 ms integration, shifting to the s2 or s3 algorithms did not result in improved performance. The s3th1 version of the algorithm, however, yielded specificity 0.94 with sensitivity 0.83. Regardless of integration time, algorithm variants that further reduced reported false positives also lead to loss in sensitivity (Table 4).

With the failure of algorithm and integration time variations for achieving desired performance metrics, we considered the array elements. The array utilized to this

http://dx.doi.org/10.1016/j.heliyon.2017.e00312

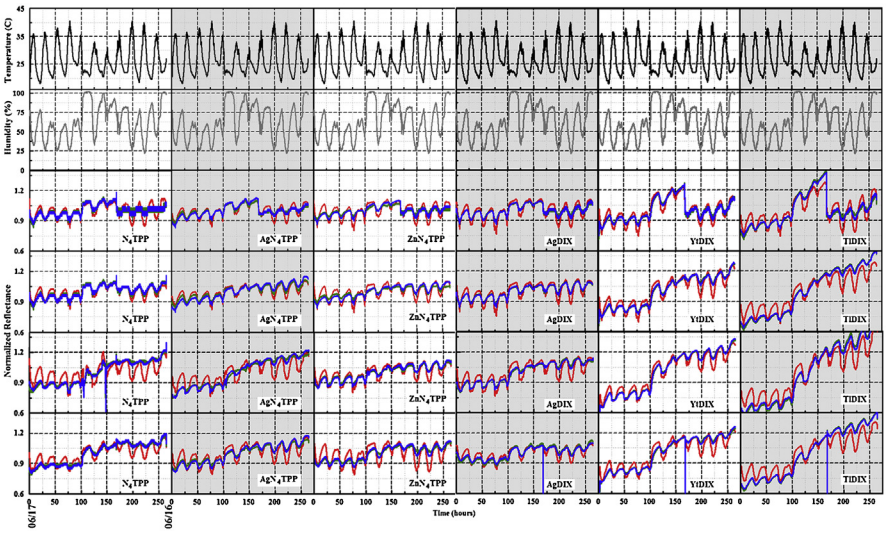

Fig. 12. Normalized RGB color value data set collected on the 11 m rooftop between June 24 and June 28, 2016 at 100, 300, 400, and 500 ms integration. Temperature (black) and humidity (grey) as reported by a co-located device are also provided.

point includes indicators that provide variable response to the three targets. It is impossible to screen for potential interactions with all possible variations that could be encountered in environmental air samples. In order to evaluate the potential for improving performance with adjustment to the array elements, we replaced the N_4TPP array element with a sample of clean WypAll X60; all other elements of the original array were retained. The WypAll was expected to provide a negative control for the device. This new array was used with 300 and 400 ms integration at the 18 m rooftop site. Table 5 provides results of analysis for the array under the algorithm variants. With the original array, the 400 ms integration duration returned specificity 0.86 and sensitivity 0.75 (0.94 and 0.83 at 300 ms) under the s3th1 algorithm. Using the array with control element, the 400 ms integration duration returned specificity 0.97 and sensitivity 1.00 (0.93 and 1.00 at 300 ms).

Additional materials, printer paper and weigh paper (Fisherbrand, Hampton, NH), were also evaluated as potential negative controls (Fig. 13 and Table 5 and Table 6). These materials were more responsive to changes in humidity than the WypAll. The performance of the devices using weigh paper as an array component was similar to those using the WypAll; printer paper showed slightly poorer performance.

4. Discussion

The study presented here demonstrates the utility of reflectance based sensing using porphyrin and metalloporphyrin indicators for environmental monitoring. Initial analysis (s1 algorithm) of the outdoor data set indicated a specificity of 0.87

http://dx.doi.org/10.1016/j.heliyon.2017.e00312

Table 5. Summary of algorithm reporting for the negative control containing arrays at 300 ms and 400 ms integration durations. This data include 145 h run time for each device. Table 6 provides detailed information on WypAll control swatch responses.

Integration Duration	True Positives	False Positives	False Negatives	True Negatives	Specificity	Sensitivity
WypAll, 300 ms integration						
s1	7	14	0	99	0.88	1.00
s2	7	13	0	95	0.88	1.00
s3	7	9	0	101	0.92	1.00
s3th1	7	10	0	125	0.93	1.00
s3th2	3	2	4	134	0.99	0.43
s3th1b	3	2	4	134	0.99	0.43
s3th2b	2	2	5	133	0.99	0.29
WypAll, 400 ms integration						
s1	7	12	0	85	0.88	1.00
s2	7	15	0	97	0.87	1.00
s3	7	14	0	107	0.88	1.00
s3th1	7	4	0	130	0.97	1.00
s3th2	4	2	3	135	0.99	0.57
s3th1b	4	2	3	135	0.99	0.57
s3th2b	1	2	6	133	0.99	0.14
Printer Paper Negative Control, 400 ms integration						
S1	7	16	0	83	0.84	1.00
S2	7	10	0	79	0.89	1.00
S3	7	9	0	86	0.91	1.00
S3th1	5	7	2	108	0.94	0.71
S3th2	5	2	2	122	0.98	0.71
S3th1b	5	2	2	122	0.98	0.71
S3th2b	5	2	2	123	0.98	0.71
Waxed Weigh Paper Negative Control, 400 ms integration						
S1	7	10	0	96	0.91	1.00
S2	7	12	0	100	0.89	1.00
S3	7	9	0	108	0.92	1.00
S3th1	7	4	0	122	0.97	1.00
S3th2	2	1	5	127	0.99	0.29
S3th1b	2	1	5	127	0.99	0.29
S3th2b	2	1	5	129	0.99	0.29

http://dx.doi.org/10.1016/j.heliyon.2017.e00312

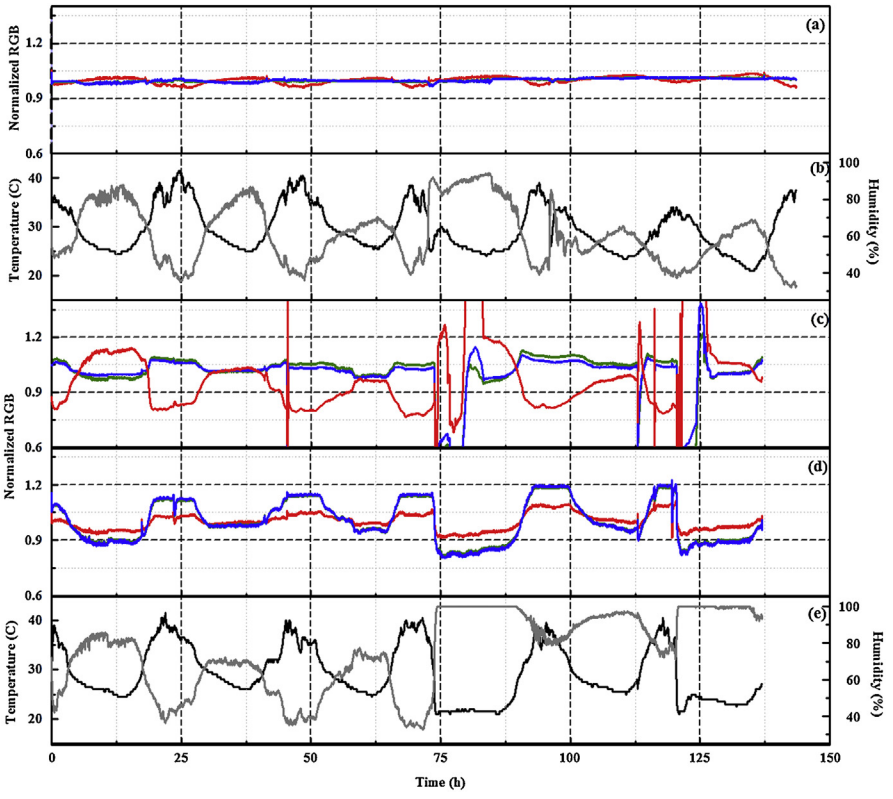

Fig. 13. Normalized RGB color value data set collected on the 18 m rooftop: (A) WypAll – July 5 and July 11, 2016 (145 h) with associated temperature and humidity (B); (C) printer paper and (D) weigh paper – July 13 to July 19, 2016 (137 h) with associated temperature and humidity (E).

with a sensitivity of 0.86. Through tuning of the algorithm parameters and re-analysis of the outdoor data set, we found that sensitivity could be improved but only at the expense of the specificity. Changing device parameters (integration time) provided the potential for improving specificity significantly (0.94) with moderate losses in specificity (0.83). Adding an indicator material that should not be sensitive to the presence of targets or interferents (untreated WypAll), provided the potential to further improve performance (specificity 0.97 and sensitivity 1.0). It is important to note that these optimizations could not be completed using an indoor data set alone [13]. A recent US Department of Defense proposal solicitation sought false alarm rates of less than one per 72 h with a stretch goal of 1 per week (168 h) [21]. The 400 ms integration data set incorporating the WypAll control indicator was comprised of 145 h of outdoor data collection. The run time to the first false response was 70 h with an average of 35 h; this time can be extended, but it is at the expense of sensitivity in the current device.

While we were able to demonstrate the potential of this sensing approach for long term environmental monitoring, initial results indicated sensitivities less than that desired for the application. We had previously completed a more detailed

http://dx.doi.org/10.1016/j.heliyon.2017.e00312

Table 6. PT4 data set from 18 m rooftop experiments (30 s increment; 400 ms integration); total run time 137 h, July 5 to July 11, 2016. Indicator 1–WypAll, indicator 2–AgN_4TPP, indicator 3–ZnN_4TPP, indicator 4 − AgDIX, indicator 5 − YtDIX, indicator 5 − TlDIX.

		s1			s3th1		
Target	**Spiked**	**Detected Begin**	**Window End**	**Indicator #**	**Detected Begin**	**Window End**	**Indicator #**
Unknown		7/5/2016 16:31	7/5/2016 17:17	5			
Unknown		7/5/2016 18:49	7/5/2016 20:27	3;4;6			
Unknown		7/6/2016 1:10	7/6/2016 4:02	4;6			
Ethanol, swab	07/06/2016 09:16	7/6/2016 9:19	7/6/2016 12:02	1;3;4;5;6	7/6/2016 9:21	7/6/2016 9:37	1;3;4;5;6
Methanol, swab	07/06/2016 12:26	7/6/2016 12:26	7/6/2016 14:38	1;3;4;5;6	7/6/2016 12:13	7/6/2016 13:38	1;2;3;4;5;6
Isopropanol, swab	07/06/2016 16:32	7/6/2016 16:33	7/6/2016 18:59	1;3;4;5;6	7/6/2016 16:36	7/6/2016 17:04	1;2;3;4;5;6
Ethanol, spray	07/07/2016 08:28	7/7/2016 8:28	7/7/2016 9:36	1;3;4;5;6	7/7/2016 8:49	7/7/2016 8:56	1;3;4;5;6
Methanol, spray	07/07/2016 10:38	7/7/2016 10:38	7/7/2016 16:44	1;2;3;4;5;6	7/7/2016 12:10	7/7/2016 13:47	1;2;3;4;5;6
Unknown		7/7/2016 18:44	7/7/2016 18:49	4			
Isopropanol, spray	07/08/2016 08:53	7/8/2016 8:53	7/8/2016 19:15	1;3;4;5;6	7/8/2016 8:53	7/8/2016 9:01	1;3;4;5;6
Unknown					7/8/2016 13:08	7/8/2016 13:22	3;4;5;6
Unknown					7/8/2016 15:53	7/8/2016 16:57	1;2;3;4;5;6
Unknown		7/9/2016 1:32	7/9/2016 1:38	4			
Unknown		7/9/2016 3:17	7/9/2016 4:34	1;3;4;6			
Unknown		7/9/2016 10:54	7/9/2016 18:50	1;2;3;4;5;6			
Unknown					7/9/2016 15:19	7/9/2016 16:35	1;2;3;4;5;6
Unknown		7/9/2016 20:49	7/9/2016 20:58	3;6			
Unknown		7/10/2016 10:35	7/10/2016 10:47	3;4;6			
Unknown		7/10/2016 11:50	7/10/2016 14:02	3;4;6			
Unknown		7/10/2016 15:13	7/10/2016 16:52	3;4;6			
Ethanol, spray	07/11/2016 08:41	7/11/2016 8:41	7/11/2016 12:42	1;3;4;5;6	7/11/2016 8:42	7/11/2016 8:51	1;3;4;5;6
Unknown		7/11/2016 14:15	7/11/2016 14:32	3;4;6			

http://dx.doi.org/10.1016/j.heliyon.2017.e00312

laboratory study using similar prototype devices [13]. This study provided highly controlled conditions allowing for detailed evaluation of algorithm performance. It was determined that changing the parameters of prototype function could have a significant impact on sensitivity. Applying those results here, the integration time was shifted from 100 ms to 400 ms. A significant improvement to specificity was achieved without losses in sensitivity. The previous study also identified the benefit of shorter sampling increments (5 s versus 30 s). A prototype device currently under development will address both considerations by providing simultaneous capture of RGB values from all indicators. This will allow the sampling increment to be fixed by the necessary integration time, rather than being fixed by a combination of integration time and total number of array elements.

While this type of sensing approach has been used previously, the applications are typically end-point or dosimetry-type rather than continuous [6, 7]. In addition, much of the previous work relies on exposure with subsequent removal of indicators for analysis by image capture, requiring significant processing power as well as additional time. The prototype devices described here are intended as a step toward long term, autonomous sensing. The envisioned application would include a network of devices communicating as needed with a central site for real-time reporting of event detection. Realization of this goal requires incorporation of communications as well as the processing algorithm into the prototype. In addition, the ongoing effort seeks to expand the number of indicator elements used in the array to increase target identification capabilities; the current device uses six. The final goal of the effort is to deploy the devices as a group. This network of devices would provide further prevention of false events through redundancy. While reporting by a single device could be questioned, a series of responses by nearby devices as a threat propagates through the monitored area would offer confirmation and increased data confidence.

Declarations

Author contribution statement

Brandy J. Johnson: Conceived and designed the experiments; Performed the experiments; Analyzed and interpreted the data; Contributed reagents, materials, analysis tools or data; Wrote the paper.

Anthony P. Malanoski: Conceived and designed the experiments; Analyzed and interpreted the data; Contributed reagents, materials, analysis tools or data; Wrote the paper.

Jeffrey S. Erickson and David A. Stenger: Contributed reagents, materials, analysis tools or data.

Ray Liu, Allison R. Remenapp and Martin H. Moore: Performed the experiments.

http://dx.doi.org/10.1016/j.heliyon.2017.e00312

Funding statement

This research was supported by the U.S. Office of Naval Research through Naval Research Laboratory base funds (69–6594).

Competing interest statement

The authors declare no conflict of interest.

Additional information

Access to raw data associated with this study may be requested by contacting the corresponding author Brandy Johnson at brandy.white@nrl.navy.mil.

Acknowledgments

Participation of R. Liu through US Navy Science and Engineering Apprenticeship Program (SEAP). Participation of A. Remenapp was supported by Washington College. We have applied the SDC approach ("sequence-determines-credit") for determining the sequence of authors [22]. The views expressed here are those of the authors and do not represent those of the U.S. Navy, the U.S. Department of Defense, or the U.S. Government.

References

[1] W. An, C. Park, X. Han, K.R. Pattipati, D.L. Kleinman, W.G. Kemple, Hidden Markov Model and Auction-Based Formulations of Sensor Coordination Mechanisms in Dynamic Task Environments, IEEE Trans. Syst. Man Cybern. A Syst. Humans 41 (6) (2011) 1092–1106.

[2] T. Gruber, L. Grim, R. Fauth, B. Tercha, C. Powell, K. Steinhardt, Implementation and testing of a sensor-netting algorithm for early warning and high confidence C/B threat detection, Proceedings SPIE, Multisensor, Multisource Information Fusion: Architectures, Algorithms, and Applications (2011).

[3] T. Gruber, L. Grim, C. Keiser, W. Ginley, Sensor-netting algorithm for CB threat mapping, A.W. Fountain Iii, P.J. Gardner (Eds.), CBRNE (2010).

[4] T. Monahan, J.T. Mokos, Crowdsourcing urban surveillance: The development of homeland security markets for environmental sensor networks, Geoforum 49 (2013) 279–288.

[5] J.R. Askim, M. Mahmoudi, K.S. Suslick, Optical sensor arrays for chemical sensing: the optoelectronic nose, Chem. Soc. Rev. 42 (22) (2013) 8649–8682.

http://dx.doi.org/10.1016/j.heliyon.2017.e00312

[6] J.R. Askim, K.S. Suslick, Hand-Held Reader for Colorimetric Sensor Arrays, Anal. Chem. 87 (15) (2015) 7810–7816.

[7] L. Feng, C.J. Musto, J.W. Kemling, S.H. Lim, K.S. Suslick, A colorimetric sensor array for identification of toxic gases below permissible exposure limits, Chem. Comm. 46 (2010) 2037–2039.

[8] M. Fox, N. Goldstein, P. Vujkovic-Cvijin, B. Gregor, S. Adler-Golden, J. Cline, B. St Peter, A. Lowell, M. Wilder, A compact thermal-infrared spectral imager for chemical-specific detection, In: P. Mouroulis, T.S. Pagano (Eds.), Imaging Spectrometry Xviii, 2013.

[9] B.J. Johnson, J.S. Erickson, J. Kim, A.P. Malanoski, I.A. Leska, S.M. Monk, D.J. Edwards, T.N. Young, J. Verbarg, C. Bovais, R.D. Russell, D.A. Stenger, Miniaturized reflectance devices for chemical sensing, Meas. Sci. Technol. 25 (9) (2014) 10.

[10] R.A. Potyrailo, Multivariable Sensors for Ubiquitous Monitoring of Gases in the Era of Internet of Things and Industrial Internet, Chem. Rev. 116 (19) (2016) 11877–11923.

[11] J.N. Sanders-Reed, Applications and challenges for MMW and THz sensors, In: T. George, A.K. Dutta, M.S. Islam (Eds.), Micro- and Nanotechnology Sensors Systems and Applications Vii, 2015.

[12] K.L. Gares, K.T. Hufziger, S.V. Bykov, S.A. Asher, Review of explosive detection methodologies and the emergence of standoff deep UV resonance Raman, J. Raman Spectrosc. 47 (1) (2016) 124–141.

[13] A.P. Malanoski, B.J. Johnson, J.S. Erickson, D.A. Stenger, Development of a detection algorithm for use with reflectance-based, real-time chemical sensing, Sensors 16 (2016) 1927.

[14] A. Hannon, Y.J. Lu, J. Li, M. Meyyappan, A Sensor Array for the Detection and Discrimination of Methane and Other Environmental Pollutant Gases, Sensors 16 (8) (2016).

[15] R. Huerta, T. Mosqueiro, J. Fonollosa, N.F. Rulkova, I. Rodriguez-Lujan, Online decorrelation of humidity and temperature in chemical sensors for continuous monitoring, Chemometr. Intell. Lab. 157 (2016) 169–176.

[16] C. Zhang, D.P. Bailey, K.S. Suslick, Colorimetric sensor arrays for the analysis of beers: A feasibility study, J. Agric. Food Chem. 54 (14) (2006) 4925–4931.

http://dx.doi.org/10.1016/j.heliyon.2017.e00312

[17] N. Maurya, S. Bhardwaj, A.K. Singh, A modest colorimetric chemosensor for investigation of CN-in semi-aqueous environment with high selectivity and sensitivity, Sens. Actuators B Chem. 229 (2016) 483–491.

[18] R. Montes-Robles, M.E. Moragues, J.L. Vivancos, J. Ibanez, R. Fraile, R. Martinez-Manez, E. Garcia-Breijo, Colorimetric detection of hazardous gases using a remotely operated capturing and processing system, Isa Trans. 59 (2015) 434–442.

[19] S.H. Park, A. Maruniak, J. Kim, G.R. Yi, S.H. Lim, Disposable microfluidic sensor arrays for discrimination of antioxidants, Talanta 153 (2016) 163–169.

[20] B.J. Johnson, R. Liu, R.C. Neblett, A.P. Malanoski, M. Xu, J.S. Erickson, L. Zang, D.S. Stenger, M.H. Moore, Reflectance-based detection of oxidizers in ambient air, Sens. Actuators B Chem. 227 (2016) 399–402.

[21] Defense Threat Reduction Agency Chemical and Biological Defense Program, Joint Science and Technology Office for Chemical and Biological Defense Service Call for Proposals FY14/16 JSTO-CBD FY14-16 Service Call, (2013) .

[22] T. Tscharntke, M.E. Hochberg, T.A. Rand, V.H. Resh, J. Krauss, Author Sequence and Credit for Contributions in Multiauthored Publications, PLoS Biol. 5 (1) (2007) e18.

http://dx.doi.org/10.1016/j.heliyon.2017.e00312